

# Courageous science: structural studies of bluetongue virus core

Michael G Rossmann\* and Yizhi Tao

The structure of the bluetongue virus core was recently reported and represents the largest structure determined to atomic resolution. As a biological machine capable of RNA transcription, the structure has immense biological significance.

Address: Department of Biological Sciences, Purdue University, West Lafayette, Indiana 47907-1392, USA.

\*Corresponding author.

E-mail: mgr@indiana.bio.purdue.edu

Structure March 1999, 7:R43–R46

<http://biomednet.com/elecref/09692126007R0043>

© Elsevier Science Ltd ISSN 0969-2126

In a recent edition of *Nature* [1], David Stuart and coworkers published the three-dimensional structure of the core of bluetongue virus. The total molecular weight of the  $\sim 700$  Å diameter particle is  $\sim 54 \times 10^6$  Da, and is by far the largest atomic structure yet to be determined by crystallographic techniques. This is a fantastic accomplishment not only for its technical achievements, but also for its biological significance in elucidating a structure capable of RNA transcription. Yet, the account has only a brief description of the crystallographic methods, and there is only scant discussion of the function of this extraordinary molecular machine. These apparent omissions are in no way the fault of the authors, however. Methodological details are missing because the basic crystallographic techniques required for solving the structure, once highly controversial [2], have become commonplace. On the other hand, discussion of the structure in terms of its known functions, in particular its ability to transcribe messenger RNA molecules within the intact core, is still sufficiently controversial that it was denied publication in *Nature*, according to the author (D Stuart, personal communication).

Bluetongue virus is an orbivirus that belongs to the reoviridae family of segmented double-stranded (ds)RNA, icosahedral viruses with two or three layers of proteins that form the capsid. The virus causes disease in cattle and, in particular, in sheep; it is endemic in the Middle East, India, China, and the western parts of the US [3]. The outer shell of orbiviruses contain a number of proteins that can recognize and interact with cell-surface molecules. These are stripped off during cell entry, leaving a viral core which has an outer layer of  $13 \times 60$  (= 780) copies of the viral protein VP7 (MW 38,000) and an inner layer of  $2 \times 60$  (= 120) VP3 viral protein subunits (MW 100,000).

The first papers on bluetongue virus from the Stuart and Roy laboratories related to the structure of VP7 on its own [4]. This protein arranges itself as trimers in a number of different crystal forms [5]. The monomer is  $\sim 85$  Å long with its length running roughly parallel to the trimer axis. The structure of the monomer has two domains: a helical domain, formed by the N- and C-terminal regions, and a 'jelly-roll' domain, formed by the central one-third of the polypeptide. It was shown that the crystallographic trimers were likely to be relevant to the structure of the virus itself and that the jelly-roll domain would form the external surface of the core. Topologically similar jelly-roll domains have been found in most, but not all, other virus capsids [6]. Electron microscopic (EM) reconstructions [7,8] were able to establish the overall organization of the proteins in bluetongue virus. This made it possible to build a fairly accurate model of the outer layer of bluetongue virus cores by fitting the VP7 trimer structures into electron-density maps generated from EM images [5]. Thus, when it became possible to crystallize bluetongue virus cores and collect three-dimensional X-ray diffraction data using various synchrotron sources, these data could be related to the proposed model. Subsequent electron-density averaging between noncrystallographically related protein subunits was able to extend and improve the effective resolution of the electron-density map, thus permitting a first view of the internal VP3 subunits in atomic detail.

The use of an homologous model and the subsequent electron-density averaging had been controversial from the time of its first proposal [9] to its eventual successful use in the structure determinations of a human rhinovirus [10] and poliovirus [11]. Since 1985, however, this technology has been used in the structure determination of numerous other viruses, as well as proteins. In commenting on the crystallographic techniques, it should also be mentioned that data acquisition when cell dimensions are 800 Å or longer is itself a substantial achievement, made possible only by numerous advances in the development of the use of synchrotron radiation sources, powerful computational facilities, and suitable software for the indexing and measurement of intensities of millions of X-ray reflections [12].

Crick and Watson [13,14] argued that the genetic code was likely to be based on somewhere between two and six bases per amino acid. Hence, it followed that the amount of information available on a viral genome would be insufficient to code for a polypeptide chain large enough to form the complete viral capsid. Instead, they suggested that a closed capsid must consist of many identical protein subunits. Being identical, each subunit should then bind

other subunits in identical ways. Thus, the environment of each subunit must be identical. The only geometric arrangements that allow this are the Platonic solids, including a tetrahedron, octahedron or icosahedron. Of these, the icosahedron requires the greatest number of asymmetric objects, namely 60, to form a complete regular figure. Although this observation has remained true for most 'spherical' viruses, it does not explain how subunits evolve to associate with each other at exactly those angles that fortuitously create an icosahedral shape. Nor is it entirely clear why no viruses have yet been discovered that have other than icosahedral symmetry, although an icosahedron would provide the largest volume for the genome with the least surface area of the capsid.

Almost a decade after Crick and Watson first proposed their ideas on virus symmetry, Caspar and Klug [15] extended these concepts to accommodate viruses that have more than 60 subunits in their capsid, as is the case in most viruses. Their argument was that if the proteins in a viral capsid do not have identical environments (which would only be possible if there were exactly 60 subunits in the capsid), the proteins must have at least roughly identical ('quasi-equivalent') environments. For instance, the conformation of a protein might be able to adapt itself to make hexamers with  $60^\circ$  between subunits or pentamers with  $72^\circ$  between subunits. A regular icosahedron can then be considered to be made up of 12 pentamers ( $12 \times 5 = 60$  subunits). But other viruses might have additional hexamers at strategic, but regularly placed, positions. Caspar and Klug showed that such quasi-equivalent arrangements could only occur when the number of subunits in the shell was  $60T$ , where the triangulation number,  $T$ , is given by  $T = h^2 + hk + k^2$ , and  $h$  and  $k$  are integers. This implies that only certain  $T$  numbers are possible. For instance,  $T = 1, 3, 4, 7, 9$ , and  $13$  are allowed, whereas  $T = 2, 5, 6, 8, 10, 11$ , and  $12$  are not. In most cases, these predictions have been found to be valid, both in terms of the number of asymmetric subunits in the particle and the organization of pentamers and hexamers in the capsid. The first truly major discrepancy was discovered in the  $T = 7$  structures of the homologous polyoma and simian virus 40 (SV40) virions [16,17]. It was found that these viruses were not built of 12 pentamers and 60 hexamers, as had been predicted by Caspar and Klug, but rather that the anticipated hexamers were, in reality, pentamers. This discovery jolted virologists out of an unquestioning acceptance of the Caspar and Klug predictions. Subsequently, Harrison and coworkers [18] showed that the N-terminal domain of the SV40 subunits within the hexavalent pentamers had adapted their conformations in a subtle way to conform to their specific environments.

The inner subcore of bluetongue virions comprises 120 subunits, a number that is disallowed by the Caspar and Klug triangulation rules. Nevertheless, the two molecules

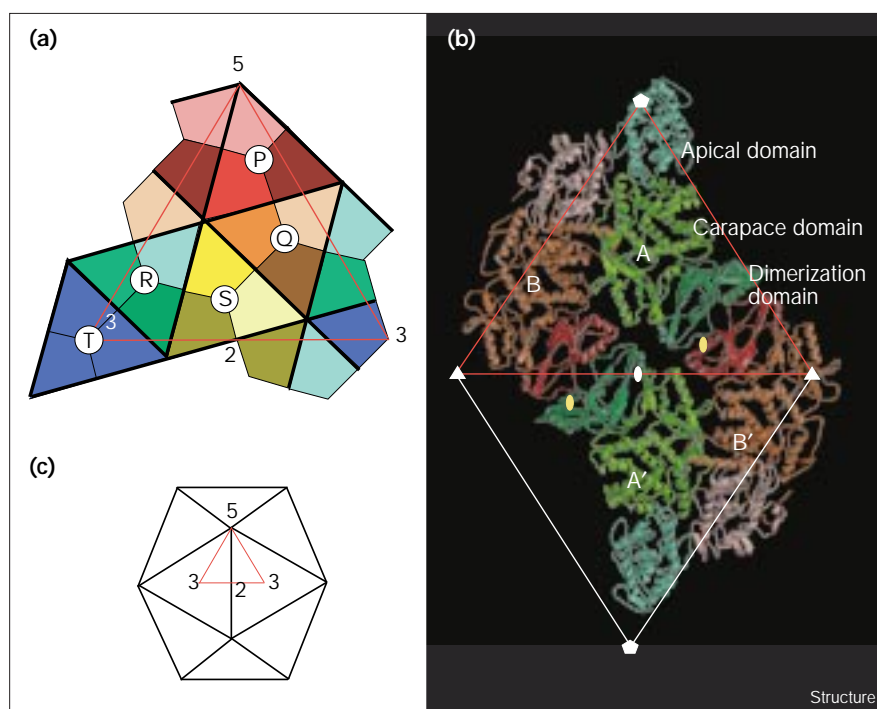
per icosahedral repeating unit adapt their conformation to their respective environments by structural changes especially in the apical domains, close to the fivefold axes (Figure 1). There is, however, also a symmetry mismatch between the non-Caspar–Klug  $T = 2$  inner core of VP3 subunits and the classical Caspar–Klug  $T = 13$  outer core of VP7 subunits (Figure 1). The 13 quasi-equivalent subunits of the outer core each have totally different, nonspecific, hydrophobic interactions with the inner core. A similar mismatch has been observed in the structure of the  $\phi$ X174 procapsid [19], where each of the four, non-Caspar–Klug arranged, scaffolding proteins per icosahedral unit has a completely different interaction with the inner core of the  $T = 1$  icosahedrally organized capsid shell. Such symmetry mismatches are found to be quite common in viruses and may be functional requirements. For example, the neck–tail connector in the tailed bacterial virus  $\phi$ 29 has 12-fold symmetry, but it fits into a fivefold vertex of the head [20]. For  $\phi$ 29, the mismatch may be essential to rotate the connector, powered by an ATPase, while packaging the genomic dsDNA into the head capsid [21], perhaps not unlike the mechanism proposed for bovine heart mitochondrial ATPase [22].

Although it is instructive to learn how different viruses circumvent the Caspar and Klug laws, it would be helpful to find a general concept that could explain the available information and predict new findings. What has been learned is that selected protein domains have a remarkable capacity to adapt themselves to provide appropriate interactions between subunits, whereas other parts of proteins retain their structure over long evolutionary time spans. But if that is the case, why retain any semblance of the Caspar and Klug organization, as suitable interactions can apparently be readily adapted? Why retain icosahedral symmetry at all? Indeed, many viruses, particularly larger enveloped viruses, lack any pretense of icosahedral symmetry, although, like human immunodeficiency virus [23], they retain local symmetric organization between adjacent capsomeres.

An alternative point of view to the Watson–Crick and Caspar–Klug symmetry concepts is the idea of conformational switching [24]. According to this concept, when two identical proteins bind to each other, they induce a conformational change in each other. Thus, when a third molecule binds to either of the first two molecules, it cannot bind in the same way because the original conformation no longer exists. The conformational changes induced on the third molecule might, therefore, be different to those induced on one or the other of the first two molecules. Hence, the path of assembly is entirely controlled by successive assembly events, in contrast to the highly successful predictions of Crick and Watson as well as those of Caspar and Klug. Furthermore, conformational switching does not explain the high symmetry of viruses. Nevertheless, the structural changes induced in the apical domains

Figure 1

The arrangement of subunits in bluetongue virus. The contents of the asymmetric unit (outlined in red) are shown (a) diagrammatically for the larger, outer ( $T=13$ ) VP7 shell and (b) as a ribbon diagram for the smaller, inner ( $T=2$ ) VP3 shell. The VP7 subunits are arranged as five trimers, P, Q, R, S, and T, with T being on an icosahedral threefold axis and P surrounding the icosahedral fivefold axes. In (a), each independent trimer of VP7 is outlined in black and given a color. The P trimer is shown in shades of red, Q in shades of brown, S in shades of yellow, R in shades of green and the T trimer is shown entirely in blue because its monomers are identical in structure, rather than merely quasi-equivalent. The two independent VP3 subunits (red and green in (b)) are related by a quasi-twofold axis, shown as a yellow oval. The different shades of green and red indicate the apical, carapace, and dimerization domains of each VP3 subunit. The symmetry mismatches between the two shells can be seen by superimposition of (a) and (b). (c) The organization of the icosahedral asymmetric unit, also outlined in red, within the icosahedral framework; the two-, three-, and fivefold axes are labeled.



of bluetongue VP3 can be ‘understood’ in terms of conformational switching. A parallel to the differing hypotheses of viral assembly is in the quantum theory of energy, where a few assumptions can explain many observations while being unable to provide any true understanding in terms of cause and effect.

The enzyme complex capable of transcription probably attaches to the innermost VP3 shell at its fivefold vertices. The transcripts are externalized by way of pores in the capsid, an event that has been beautifully captured in an EM study [25] of a related rotavirus. Grimes *et al.* [1] observed that the most likely pores through which the transcribed RNA might escape from the virion are channels along the fivefold axes. However, this route would require large conformational changes to widen these apertures in the VP3 capsid. This has analogies with the probable function of fivefold axes in rhinoviruses and parvoviruses, as well as the insect Flock House virus. Rhinoviruses and Flock House virus externalize their genomic RNA, probably through selected fivefold channels, while infecting cells [26,27]; parvoviruses externalize the N-terminal domain of their capsid proteins through the fivefold channel, a process that may be essential for viral maturation [28].

Lipid-enveloped bacterial viruses [29], such as  $\phi 6$ , have many similarities to mammalian reoviruses. They have an outer shell of  $T=13$  and an inner core of  $T=2$  symmetry [30]. These viruses have only three segments of RNA,

however, instead of the ten observed in bluetongue virus. Mindich and colleagues have shown, in a series of elegant experiments, that the three RNA segments of lipid-enveloped viruses are packaged in a specific order [31]. Conformational switching may, therefore, be the process by which procapsids sequentially select each of the ten different dsRNA segments in bluetongue virus. In contrast, transcription of each RNA molecule appears to occur simultaneously, and this may be related to the organization of the transcription complexes around each of the 12 pentameric sites within the core [1].

The structure of the bluetongue virus core has now provided ample opportunities for constructive interpretation of the way in which this amazing biological machine functions. We hope that David Stuart and his colleagues will soon have the opportunity to publish their interpretation of how the bluetongue virus functions as a transcription machine.

#### Acknowledgements

We thank Sharon Wilder for helpful comments.

#### References

1. Grimes, J.M., *et al.*, & Stuart, D.I. (1998). The atomic structure of the bluetongue virus core. *Nature* **395**, 470-478.
2. Rossmann, M.G. (1972). Introduction. In *The Molecular Replacement Method*. (Rossmann, M.G., ed.), pp. 4-15, Gordon & Breach, New York.
3. Monath, T.P. & Guirakhoo, F. (1996). Orbiviruses and coltivirus. In *Fields Virology*. (Fields, B.N., Knipe, D.M. & Howley, P.M., eds.), Vol. 2, pp. 1735-1766, Lippincott-Raven Publishers, Philadelphia.
4. Grimes, J., Basak, A.K., Roy, P. & Stuart, D. (1995). The crystal structure of bluetongue virus VP7. *Nature* **373**, 167-170.

5. Grimes, J.M., *et al.*, & Prasad, B.V.V. (1997). An atomic model of the outer layer of the bluetongue virus core derived from X-ray crystallography and electron microscopy. *Structure* **5**, 885-893.
6. Rossmann, M.G. & Johnson, J.E. (1989). Icosahedral RNA virus structure. *Annu. Rev. Biochem.* **58**, 533-573.
7. Prasad, B.V.V., Yamaguchi, S. & Roy, P. (1992). Three-dimensional structure of single-shelled bluetongue virus. *J. Virol.* **66**, 2135-2142.
8. Hewat, E.A., Booth, T.F. & Roy, P. (1994). Structure of correctly self-assembled bluetongue virus-like particles. *J. Struct. Biol.* **112**, 183-191.
9. Rossmann, M.G. & Blow, D.M. (1962). The detection of sub-units within the crystallographic asymmetric unit. *Acta Crystallogr.* **15**, 24-31.
10. Rossmann, M.G., *et al.*, & Vriend, G. (1985). Structure of a human common cold virus and functional relationship to other picornaviruses. *Nature* **317**, 145-153.
11. Hogle, J.M., Chow, M. & Filman, D.J. (1985). Three-dimensional structure of poliovirus at 2.9 Å resolution. *Science* **229**, 1358-1365.
12. Sawyer, L., Isaac, N. & Bailey, S. (1993). *Data Collection and Processing, Proceedings of the CCP4 Study Weekend, 29-30 January 1993*. SERC Daresbury Laboratory, Warrington, UK.
13. Crick, F.H.C. & Watson, J.D. (1956). Structure of small viruses. *Nature* **177**, 473-475.
14. Crick, F.H.C. & Watson, J.D. (1957). Virus structure: general principles. In *Ciba Foundation Symposium on 'The Nature of Viruses'*. (Wolstenholme, G.E.W. & Millar, E.C.P., eds.), pp. 5-13, Little Brown & Co., Boston.
15. Caspar, D.L.D. & Klug, A. (1962). Physical principles in the construction of regular viruses. *Cold Spring Harbor Symp. Quant. Biol.* **27**, 1-24.
16. Rayment, I., Baker, T.S., Caspar, D.L.D. & Murakami, W.T. (1982). Polyoma virus capsid structure at 22.5 Å resolution. *Nature* **295**, 110-115.
17. Baker, T.S., Drak, J. & Bina, M. (1988). Reconstruction of the three-dimensional structure of simian virus 40 and visualization of the chromatin core. *Proc. Natl Acad. Sci. USA* **85**, 422-426.
18. Liddington, R.C., Yan, Y., Moulai, J., Sahli, R., Benjamin, T.L. & Harrison, S.C. (1991). Structure of simian virus 40 at 3.8 Å resolution. *Nature* **354**, 278-284.
19. Dokland, T., *et al.*, & Rossmann, M.G. (1997). Structure of a viral procapsid with molecular scaffolding. *Nature* **389**, 308-313.
20. Tao, Y., Olson, N.H., Xu, W., Anderson, D.L., Rossmann, M.G. & Baker, T.S. (1998). Assembly of a tailed bacterial virus and its genome release studied in three dimensions. *Cell* **95**, 431-437.
21. Hendrix, R.W. (1998). Bacteriophage DNA packaging: RNA gears in a DNA transport machine. *Cell* **94**, 147-150.
22. Abrahams, J.P., Leslie, A.G.W., Lutter, R. & Walker, J.E. (1994). Structure at 2.8 Å resolution of F<sub>1</sub>-ATPase from bovine heart mitochondria. *Nature* **370**, 621-628.
23. Fuller, S.D., Wilk, T., Gowen, B.E., Kräusslich, H.G. & Vogt, V.M. (1997). Cryo-electron microscopy reveals ordered domains in the immature HIV-1 particle. *Curr. Biol.* **7**, 729-738.
24. Kellenberger, E. (1976). Cooperativity and regulation through conformational changes as features of phage assembly. *Phil. Trans. Roy. Soc. Lond. B* **276**, 3-13.
25. Lawton, J.A., Estes, M.K. & Prasad, B.V.V. (1997). Three-dimensional visualization of mRNA release from actively transcribing rotavirus particles. *Nat. Struct. Biol.* **4**, 118-121.
26. Giranda, V.L., *et al.*, & Rueckert, R.R. (1992). Acid-induced structural changes in human rhinovirus 14: possible role in uncoating. *Proc. Natl Acad. Sci. USA* **89**, 10213-10217.
27. Bothner, B., Dong, X.F., Bibbs, L., Johnson, J.E. & Siuzdak, G. (1998). Evidence of viral capsid dynamics using limited proteolysis and mass spectrometry. *J. Biol. Chem.* **273**, 673-676.
28. Tsao, J., *et al.*, & Parrish, C.R. (1991). The three-dimensional structure of canine parvovirus and its functional implications. *Science* **251**, 1456-1464.
29. Bamford, D.H. & Wickner, R.B. (1994). Assembly of double-stranded RNA viruses: bacteriophage φ6 and yeast virus L-A. *Sem. Virol.* **5**, 61-69.
30. Butcher, S.J., Dokland, T., Ojala, P.M., Bamford, D.H. & Fuller, S.D. (1997). Intermediates in the assembly pathway of the double-stranded RNA virus φ6. *EMBO J.* **16**, 4477-4487.
31. Qiao, X., Casini, G., Qiao, J. & Mindich, L. (1995). In vitro packaging of individual genomic segments of bacteriophage φ6 RNA: serial dependence relationships. *J. Virol.* **69**, 2926-2931.